

## Modulation of Amyloid- $\beta$ Conformation by Charge State of N-Terminal Disordered Region \*

XI Wen-Hui(郗文辉), LI Wen-Fei(李文飞)\*\*, WANG Wei(王伟)

National Laboratory of Solid State Microstructure, and Department of Physics, Nanjing University, Nanjing 210093

(Received 3 May 2012)

Based on molecular dynamics simulations, we show that variations of the charge states of the histidines, which are the main effects of pH-value change and metal binding, can lead to a drastic change of the intra-peptide interactions of the segment 17–42 and the conformational distribution of the monomeric amyloid- $\beta$  ( $A\beta$ ). Since we already knew that the conformational distribution of monomeric  $A\beta$  can largely affect  $A\beta$  fibrillar aggregation, our results suggest that the pH value change and metal binding can affect the  $A\beta$  aggregation by much more complex mechanism than just affecting the inter-peptide interactions. To fully understand the mechanism of metal binding and pH-value induced  $A\beta$  aggregation, we also need to consider their effects on the conformational distribution of monomeric  $A\beta$ .

PACS: 87.15.nr, 87.15.-v, 31.15.xv

DOI: 10.1088/0256-307X/29/8/088702

Amyloid- $\beta$  ( $A\beta$ ) is a peptide consisting of  $\sim 42$  residues. Mounting evidence suggests that fibrillar aggregation of  $A\beta$  is involved in the pathogenesis of Alzheimer's disease (AD).<sup>[1]</sup> Therefore, it has received wide attention in recent years.<sup>[2,3]</sup> Detailed structural and spectroscopic studies have shown that the fibrillar aggregates of  $A\beta$  are featured by cross- $\beta$  structure.<sup>[4,5]</sup> However, only the residues from 17 to 42 have a well-formed cross- $\beta$  structure; the residues from 1 to 16 are mostly unstructured.<sup>[4]</sup> On the contrary, the whole chain of monomeric  $A\beta$  is unstructured in aqueous solvent.<sup>[6]</sup> Apparently, during fibrillar aggregation, the  $A\beta$  peptides undergo a conformational transition from unstructured conformation to  $\beta$ -strand conformation.<sup>[7]</sup> It is interesting to investigate which factors contribute to the conformational transition and fibrillization.<sup>[8]</sup> Molecular simulations with atomic details, which are proven successful in elucidating the molecular mechanisms of the biological processes,<sup>[9,10]</sup> have been widely used in understanding the  $A\beta$  fibrillar aggregation.<sup>[11–14]</sup>

A number of experimental data showed that the  $A\beta$  fibrillar aggregation is sensitive to the pH value of the solvent<sup>[15–17]</sup> and the metal binding.<sup>[18–20]</sup> Both metal binding and relatively acidic solvents can promote aggregation. However, the related molecular mechanism is largely unclear. Near the neutral pH environment, histidine is the most sensitive pH sensor.<sup>[15]</sup> Meanwhile, the histidines are the most important metal binding sites. The metal ions affect the conformational distributions of proteins for multiple reasons, including the conformational restrictions and electrostatic interactions.<sup>[19]</sup> According to the experimental results,<sup>[15]</sup> the pKa of the histidines in  $A\beta$

are around 6.5, which suggests that in physiological conditions, around 30% of the histidines are double-protonated. On the other hand, when the metal ion was bound to the histidine, the second nitrogen hydrogen ( $H_\delta$  or  $H_\epsilon$ ) is fully deprotonated due to the strong oxidative activity of divalent metal ions. Consequently, the binding of metal ions changes the charge states of the histidines to some extent. As a result, one of the major consequences of the metal binding to histidines and the protonation/deprotonation of histidines is the modification of the charge states of the histidines. In  $A\beta$ , there are three histidines (His6, His13, and His14), and all are located at the N-terminal disordered region. Previously, people often assumed that the metal binding and pH value variation affect the  $A\beta$  fibrillar aggregation by altering the inter-peptide interactions of the disordered region.<sup>[21]</sup> Therefore, in the simulation works by molecular dynamics (MD), the N-terminal disordered parts were often removed directly.

Due to the sensitivity of the  $A\beta$  fibrillar aggregations to the pH value and metal binding, it is reasonable to consider the possibility that the N-terminal disordered part can affect the conformational distribution of the segment 17–42, and therefore participate in the  $A\beta$  fibrillar aggregation. Such an effect of the N-terminal disordered region can be modulated by the charge states of the histidines, therefore they are sensitive to the pH value and metal binding.

In this Letter, we investigate the possible effects of the N-terminal disordered part on the conformational distributions of the segment 17–42 and its modulation by the charge states of the histidines by performing replica exchange molecular dynamics (REMD) simu-

\*Supported by the National Natural Science Foundation of China under Grant Nos 91127026 and 11111140012, the Natural Science Foundation of Jiangsu Province under Grant Nos BK2011546 and BK2009008, and PAPD.

\*\*Corresponding author. Email: wfli@nju.edu.cn

© 2012 Chinese Physical Society and IOP Publishing Ltd

lations for the full length of A $\beta$  peptide. Our results show that the N-terminal residues 1–16 have a drastic effect on the conformational distributions of the segment 17–42. Meanwhile, such an effect can be modulated by the charge states of the histidines. Our results are important in understanding the mechanism of the pH value and metal ion regulated A $\beta$  fibrillar aggregation.

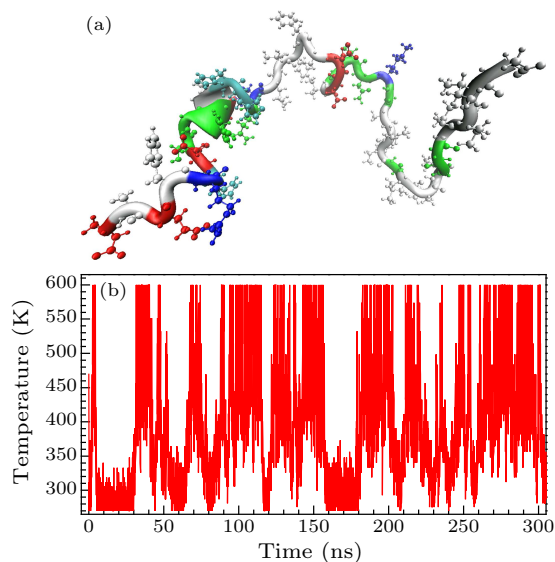


**Fig. 1.** (a) Initial structure of A $\beta$ 1–42. The residues were coloured as their type: white, nonpolar; green, polar; blue, positively charged; red, negatively charged. (b) Temperature as a function of time for a representative replica in REMD simulation.

The AMBER 11 package<sup>[22]</sup> was used to perform the simulations with the ff99SB force field.<sup>[23]</sup> In order to enhance the conformational sampling, the REMD Method was employed.<sup>[24–29]</sup> The solvent was considered implicitly with the generalized Born (GB) model.<sup>[30]</sup> In the simulations, one of the three histidines was protonated on atom N $\delta$ , which corresponds to the weak acidic conditions. As a control, we also conducted simulations with all of the histidines being neutrally charged; simulations for the system containing only the segment 17–42 were also conducted for comparisons.

The temperatures of the REMD simulations range from 270 K to 600 K and are distributed exponentially among the 32 replicas. Before the REMD simulations, each initial structure was minimized by 2000 steps and then heated up to 600 K during 5 ns. The resulting structure was used as the initial structure of REMD simulations. Figure 1(a) shows one of the initial structures of A $\beta$ 1–42. We used SHAKE algorithm<sup>[31]</sup> to constrain the covalent bonds involving hydrogen atoms. A time step of 2 fs was used. Every 1.5 ps, the replicas make an attempt to exchange conformations according to the Metropolis criteria, and the atom coordinates were saved every 0.75 ps. The simulation

for each replica was conducted for around 300 ns; the structures of the first 60 ns were omitted in the analysis. The resulting exchange rate varied from 0.32 to 0.65 with an average of 0.48. As an example, Fig. 1(b) shows the temperature as a function of time for a representative replica. The wide temperature range covered by the replica suggests the reasonable sampling quality of the REMD simulations. The convergence of the simulations was tested by calculating the errors of the calculated quantities among different time regions.

To characterize the conformational features of the peptide, we used the  $\beta$ -propensity. It was well established that the preformation of the aggregation-prone conformations can significantly speed up the fibrillar aggregation, and the aggregation-prone conformations are featured by the high populations of the  $\beta$ -strand. The PROSS algorithm, in which, based on the dihedral angles of the main chain, only the secondary structures are assigned, was used to calculate the  $\beta$ -propensity for each of the residues.<sup>[33]</sup> All analyses below are performed at 312.07 K, which is close to the physiological temperature among the 32 temperatures of the replicas.

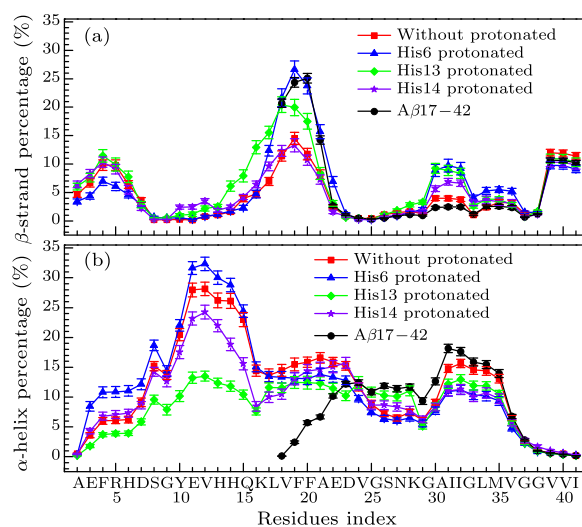


**Fig. 2.** Percentage of  $\beta$ -strand (a) and  $\alpha$ -helix (b) conformation for each of the residues in A $\beta$  peptide at different protonation states. Colour code: red, neutral state; blue, His 6 was protonated; green, His 13 was protonated; purple, His 14 was protonated. For comparison, the result for the segment 17–42 is also shown (black).

Figure 2(a) shows the percentage of  $\beta$ -strand for each of the residues at different protonation states. For comparison, the result for the segment 17–42 is also shown. The small error bars suggest a reasonable convergence of the REMD simulations. By comparing the results of the segment 17–42 and those of the full length peptide, we can see that segment 1–16 can significantly change the  $\beta$ -propensities of the residues in the segment 17–42. This effect for the residues 17–21 and 30–36 are particularly drastic. The N-terminal

residues 1–16 decreases the  $\beta$ -strand propensity in segment 17–21, while it increases that in segment 30–36. Meanwhile, the  $\beta$ -propensities of the residues of the region 17–42 can be modulated by the charge states of the histidines. By comparing with the results of the neutral state (red square), we can see clearly that the  $\beta$ -propensity was enhanced for the segments 17–21 and 30–36 when His6 (blue triangle) or His13 (green diamond) was protonated. On the contrary, the protonation of His14 (purple star) has no noticeable effect. We calculated the percentages of  $\alpha$ -helix and PPII for each of the residues at different protonation states. The results for  $\alpha$ -helix are shown in Fig. 2(b). We find that the propensities of  $\alpha$ -helix and PPII can also be largely modulated by the charge states of the histidines.

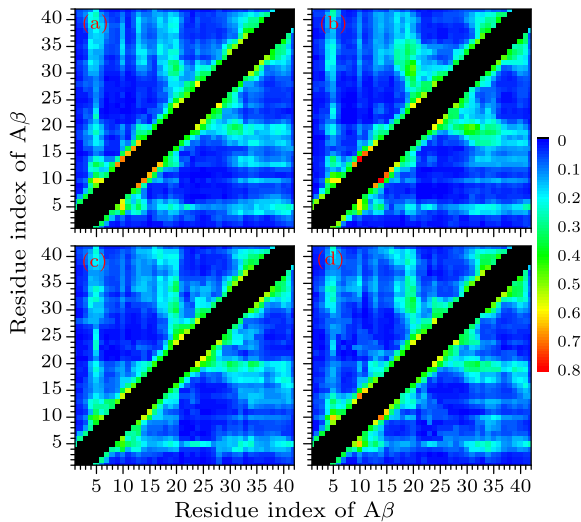


**Fig. 3.** Contact map at different protonation states: (a) neutral state, (b) His6 protonated, (c) His13 protonated, and (d) His14 protonated.

The above results reveal that residues 1–16, which are disordered in the fibrillar aggregates, have a drastic influence on the conformational distribution of residues 17–42. Such effects can be modulated by the charge states of the histidines. These results suggest that the variation of the intra-peptide interactions due to the change of the charge states of the histidines in the N-terminal disordered region can contribute to the observed pH dependence of the A $\beta$  fibrillar aggregation. Therefore, to understand to pH effect of the A $\beta$  fibrillar aggregation by MD simulations, the full length A $\beta$  should be included in the simulations.

To further understand the effects of the charge states of the histidines on the conformational distributions of the A $\beta$  peptide, we examined the formation probabilities of the intra-peptide contacts between each of the residues. A contact was considered to be formed when the distance of any heavy atoms in two residues separated by at least 3 amino acids was less than 5.0 Å. In Fig. 3, the contact maps

are shown for the simulations with different histidine charge states. From Fig. 3, we can see that the intra-peptide contacts can be affected by the charge states of the histidines, and such an effect depends on the site of the protonated histidine. Particularly, when the His6 was protonated, the anti-parallel  $\beta$ -strand was formed to a large extent between the segments 16–22 and 27–34. This result is affirmative with the above  $\beta$ -propensity analysis, which shows a high  $\beta$ -propensity for the residues of these regions. Compared to the simulations with His6 protonated, the effects for the simulations with His13 or His14 protonated are relatively weaker.

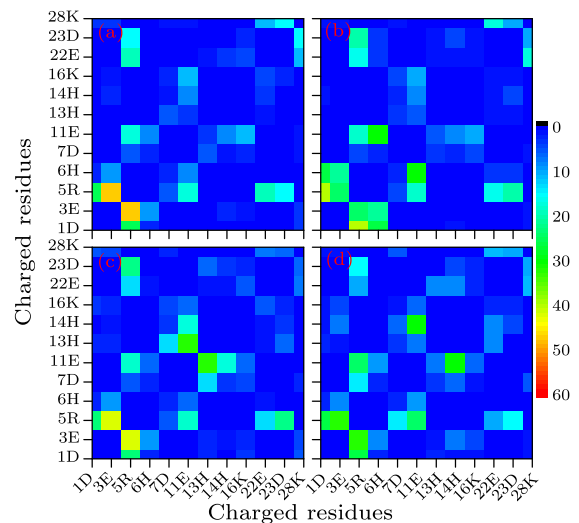


**Fig. 4.** Salt bridge map at different protonation states: (a) neutral state, (b) His6 protonated, (c) His13 protonated, and (d) His14 protonated.

As the change of the protonation states of histidines can lead to modifications of the charge distribution and electrostatic interactions, it is interesting to investigate the effects of the charge states of the histidines on the interactions between the charged residues. A number of experimental and simulation work suggested that the intra-peptide or inter-peptide salt bridges can contribute to the A $\beta$  fibrillar aggregation.<sup>[4,7]</sup> Therefore, we calculated the formation probabilities of the salt bridges between all of the charged residues and histidines. A salt bridge is regarded as formed when the distance between charged heavy atoms on the side-chains of relevant acidic and alkaline residues was less than 5.0 Å. Figure 4 shows the salt bridge maps for the simulations with different charge states. Similarly, we observed a drastic change of the formation probabilities of the salt bridges. For example, when His6 is protonated, the formation probability of the Glu22-Lys28 salt bridge was enhanced, but the formation probability of Asp23-Lys28 was reduced. In comparison, when the His13 is protonated, the formation probabilities for both the Glu22-Lys28 and the Asp23-Lys28

salt bridges are reduced. The formation probabilities for other salt bridges, including His14-Asp23, Arg5-Glu11, and Arg5-Glu22/Asp23 etc., can also be affected by changing the charge states of the histidines.

In summary, our simulation results demonstrated that the N-terminal segment, which includes residues 1–16 and is disordered in the fibrillar aggregates, can affect the conformational distributions of the residues 17–42. Such an effect can be further modulated by the charge states of the three histidines. These results suggest that modifications of the intra-peptide interactions due to the variations of the charge states of the histidines can contribute to the experimentally observed pH/metal effect of the A $\beta$  fibrillar aggregation. In addition, our results suggest that the full length A $\beta$  peptide needs to be included in the simulation system in order to reliably understand the molecular mechanism of the A $\beta$  fibrillar aggregation and its pH/metal dependences by MD simulations.

Note that although the current simulations clearly show the effects of the charge states of the histidines on the conformational distributions of the A $\beta$  peptide, we cannot establish the quantitative relationship between the pH values and the A $\beta$  fibrillar aggregation based on the current simulation results. To more clearly reveal the molecular mechanism of the pH effect of the A $\beta$  fibrillar aggregation, constant pH MD simulations for a system including a number of A $\beta$  peptides are needed, which are what is currently undergoing in our group.

## References

- [1] Selkoe D J 2001 *Physiol. Rev.* **81** 741
- [2] Hardy J and Selkoe D J 2002 *Science* **297** 353
- [3] Laferla F M, Green K N and Oddo S 2007 *Nat. Rev. Neurosci.* **8** 499
- [4] Luhers T et al 2005 *Proc. Natl. Acad. Sci. U.S.A.* **102** 17342
- [5] Tycko R 2011 *Annu. Rev. Phys. Chem.* **62** 279
- [6] Wood G P F, Rothlisberger U 2011 *J. Chem. Theor. Comput.* **7** 1552
- [7] Straub J E and Thirumalai D 2011 *Annu. Rev. Phys. Chem. U.S.A.* **62** 437
- [8] Rauk A 2009 *Chem. Soc. Rev.* **38** 2698
- [9] Zhang Z, Shi Y and Liu H 2003 *Biophys. J.* **84** 3583
- [10] Chen C and Xiao Y 2010 *J. Comput. Chem.* **31** 1368
- [11] Khandogin J and Brooks C L 2007 *Proc. Natl. Acad. Sci. U.S.A.* **104** 16880
- [12] Li W F et al 2007 *J. Phys. Chem. B* **111** 13814
- [13] Zheng J et al 2007 *Biophys. J.* **93** 3046
- [14] O'Brien E P et al 2009 *J. Phys. Chem. B* **113** 14421
- [15] Ma K et al 1999 *J. Am. Chem. Soc.* **121** 8698
- [16] Klajnert B, Cladera J and Bryszewska M 2006 *Biomacromolecules* **7** 2186
- [17] Peralvarez-Marin A, Barth A and Graslund A 2008 *J. Mol. Biol.* **379** 589
- [18] Drago D, Bolognin S and Zatta P 2008 *Curr. Alzheimer Res.* **5** 500
- [19] Jing Y Q and Han K L 2010 *Expert. Opin. Drug Discov.* **5** 33
- [20] Tougu V, Tiiman A and Palumaa P 2011 *Metallomics*. **3** 250
- [21] Miller Y, Ma B Y and Nussinov R 2010 *Proc. Natl. Acad. Sci. U.S.A.* **107** 9490
- [22] Case D A et al 2010 *Amber* (San Francisco: University of California) p 11
- [23] Duan Y et al 2003 *J. Comput. Chem.* **24** 1999
- [24] Sugita Y and Okamoto Y 1999 *Chem. Phys. Lett.* **314** 141
- [25] Zhou R H 2004 *J. Mol. Graph.* **22** 451
- [26] Zhang J, Qin M and Wang W 2006 *Proteins* **62** 672
- [27] Li W, Zhang J and Wang W 2007 *Proteins* **67** 338
- [28] Li W F, Zhang J, Wang J and Wang W 2008 *J. Am. Chem. Soc.* **130** 892
- [29] Li W F, Qin M, Tie Z X and Wang W 2011 *Phys. Rev. E* **84**
- [30] Qiu D, Shenkin P S, Hollinger F P and Still W C 1997 *J. Phys. Chem. A* **101** 3005
- [31] Ryckaert J P, Ciccotti G and Berendsen H J C 1977 *J. Comput. Phys.* **23** 327
- [32] Srinivasan R and Rose G D 1999 *Proc. Natl. Acad. Sci. U.S.A.* **96** 14258